ELSEVIER

Journal of Power Sources 79 (1999) 256–261

JOURNAL OF POWER SOURCES

Preparation and characterization of $LiNiO_2$ synthesized from $Ni(OH)_2$ and $LiOH \cdot H_2O$

H.X. Yang *, Q.F. Dong, X.H. Hu, X.P. Ai, S.X. Li

Department of Chemistry, Wuhan University, Wuhan, 430072, China

Received 25 January 1999; accepted 2 February 1999

Abstract

Synthesis of $LiNiO_2$ by heat-treatment of $Li(OH) \cdot H_2O$ and $Ni(OH)_2$ is reported. The influence of synthesis conditions on the electrochemical performance of the resulting $LiNiO_2$ is investigated. Thermal analysis of the synthesis process shows that $LiNiO_2$ formation proceeds through the transformation of $Ni(OH)_2$ to a layered compound $Ni_{1-x}(OH)_{2-x}$, followed by solid reaction with LiOH. The most favorable condition is heating a mixture of $Li(OH) \cdot H_2O$ and $Ni(OH)_2$ at 650°C, and then at 720°C in oxygen. The resulting $LiNiO_2$ exhibits a considerably high discharge capacity of 145 mA h g^{-1} and a sufficiently long cycle-life when cycled over a lithium composition range of $0.2 \leq x \leq 0.65$.

Keywords: Lithiated nickel oxide; Cathode material; Synthesis methods; Lithium-ion cells

1. Introduction

Cathode materials presently used in lithium ion cells are mainly $LiCoO_2$, $LiNiO_2$ and Li_xMnO_2, or their derivatives. Among these compounds, $LiNiO_2$ is a good compromise between electrochemical performance and material cost when compared with the poorer cycleability of Li_xMnO_2 and the higher cost of $LiCoO_2$. One reason for the limited use of $LiNiO_2$ in commercial lithium-ion cells is probably the difficulties encountered in its synthesis on large-scale production.

In recent years, many efforts have been made to develop technical methods for $LiNiO_2$ preparation. An early method described in Refs. [1–3] used a mixture of NiO and LiOH to produce $LiNiO_2$ by a solid reaction at about 700°C in air. The resulting product has a formula very close to $LiNiO_2$. Later, Ohzuku et al. [4] reported a different synthesis route in which $LiNO_3$ and $NiCO_3$ (or $Ni(OH)_2$) were selected as precursors and heat treatment was carried out under a flow of oxygen. About the same time, Kanno et al. [5] made $LiNiO_2$ through a thermal reaction of Li_2O_2 and NiO in an oxygen atmosphere. Similarly, Rongier et al. [6] obtained $Li_{0.98}Ni_{1.02}O_2$ by heating a mixture of Li_2O and NiO at 700°C. Though a number of studies has been undertaken to elucidate the influence of raw materials, atmosphere and heating temperature on the structural as well as electrochemical properties of $LiNiO_2$, there still remains some uncertainty on the detailed chemistry of the synthesis process.

In this paper, we report the synthesis of $LiNiO_2$ by thermal reaction of $Ni(OH)_2$ and LiOH and investigate the chemistry during the synthesis process and the electrochemistry behaviour of the $LiNiO_2$.

2. Experimental

2.1. Synthesis and characterization of $LiNiO_2$

The synthetic procedure is also based on a solid reaction similar to those described in [1–6], the main difference is the use of spheroidal $Ni(OH)_2$ and $LiOH \cdot H_2O$ as raw materials. The nickel and lithium hydroxide powders, in a molar ratio of Li:Ni = 1:1, were mixed uniformly by grinding in a ball mill and were then pressed into dense pellets. The heat treatment consisted of two steps: (i) heating the pellets at about 650°C for 8 to 10 h: (ii) raising the temperature to 700–800°C for 15 h in oxygen or air.

The thermal and chemical changes in the synthetic process were investigated by thermogravimetric (TG) and differential scanning calorimetry (DSC). The TG and DSC

* Corresponding author. Fax: +86-27876-47617; E-mail: hxyang@public.wh.hb.cn

0378-7753/99/$ - see front matter
PII: S0378-7753(99)00158-5

measurements were performed on 25 g samples of $LiOH \cdot H_2O$ and $Ni(OH)_2$ at 20°C min^{-1} under an oxygen or an air purge by means of a PRT2 type thermal analyzer (Beijing Optical Instrument Factory, China).

The crystalline features of the resulting $LiNiO_2$ (in powder form) were characterized by X-ray diffraction (XRD) on a RigaKu RU-200B type diffractometer with Cu K_a radiation.

The average degree of oxidation of nickel in $LiNiO_2$ was determined according to the method reported in [7]. The total amount of nickel in $LiNiO_2$ was measured by EDTA titration of a diluted hydrochloride solution of $LiNiO_2$. The oxidation state of nickel was determined by dissolution and reduction of $LiNiO_2$ to Ni^{2+} ions in dilute H_2SO_4 solution with excess ferrous ammonium sulfate and then by back titration to determine the Fe^{2+} residue with standard potassium dichromate.

2.2. Electrochemical measurements

The cyclic voltammetry of $LiNiO_2$ was carried out by use of a powder microelectrode. Fabrication of the powder microelectrode has been described in [8]. Since the current passing through the microelectrode is sufficiently small, the voltammetry can be conducted with two electrodes. Silver wires covered with AgO served as the counter and the reference electrodes.

The charge–discharge behaviour of a $LiNiO_2$ cathode was examined in experimental cells with a sandwiched design. The $LiNiO_2$ cathode was prepared by rolling the electrode paste into a 0.2-mm-thick film and pressing it on to screened A1 foil. The cathode had a composition of 85% $LiNiO_2$, 8% carbon black, and 7% PTFE. The electrolyte was 1 M $LiClO_4$ PC + DME (1:1 by vol.). The separator was a Celguard 2400 microporous polylene membrane.

Changes in the crystalline structure of the cathode during charge–discharge cycling were examined by ex-situ XRD analysis. The cathodes at the required depth of charge or discharge were removed from the experimental cells, rinsed with pure DME solvent, and transferred in a desiccator to a dry-air glove box.

3. Results and discussions

3.1. Optimization of synthesis conditions

It is well known that the performance of $LiNiO_2$ strongly depends on the choice of starting materials, the atmosphere and the heating sequences [1–6,9–11]. In terms of industrial production, the cost of the raw materials and the preparation process would also be an important factor.

A comparison of the initial capacity of $LiNiO_2$ synthesized from different combinations of lithium and nickel compounds, is given in Table 1. The data show that $LiNiO_2$ obtained from $Li(OH) \cdot H_2O$ and $Ni(OH)_2$ not only have the highest discharge capacity (135 mA h g^{-1}), but also have the highest charge–discharge efficiency. On the other hand, both LiOH and $Ni(OH)_2$ are cheap and chemically stable materials and use of the compounds does not involve the production of any harmful side-products during the synthesis process. Thus, it appears better to use LiOH and $Ni(OH)_2$ for industrial preparation of $LiNiO_2$.

Table 1
Initial capacity of $LiNiO_2$ samples synthesized from different combinations of various lithium and nickel salts

Starting compounds	Initial charge–discharge capacity (mA h g^{-1})	Charge–discharge efficiency (%)
$2LiOH \cdot H_2O + Ni_2O_3$	150–103	68.67
$LiOH \cdot H_2O + Ni(OH)_2$	175–135	77.14
$LiOH \cdot H_2O + NiC_2O_4$	140–100	71.43
$Li_2CO_3 + Ni_2O_3$	120–65	54.17
$Li_2CO_3 + 2Ni(OH)_2$	165–110	66.67
$Li_2CO_3 + 2NiC_2O_4$	135–90	66.67
$2NiNO_3 + Ni_2O_3$	180–110	61.11
$NiNO_3 + Ni(OH)_2$	150–95	63.33
$NiNO_3 + NiC_2O_4$	135–90	66.67

Synthesis conditions: heat at 650°C for 9 h, then at 720°C for 15 h in oxygen.

The influence of heating temperature and atmosphere on the initial capacity of $LiNiO_2$ is shown in Table 2. Samples prepared in air at a temperature below 650°C yield little charge and discharge capacity, viz., 55 and 20 mA h g^{-1}, respectively. With increasing temperature, the discharge capacity of samples made in air increases rapidly, but the maximum value is only 85 mA h g^{-1}. By contrast, samples prepared in oxygen exhibit a remarkable improvement in charge–discharge behaviour, the discharge capacity exceeds 130 mA h g^{-1} at the 0.4 C rate. The data in Table 2 also demonstrate that the electrochemical performance of the samples is very sensitive to the upper limit of temperature assigned to $LiNiO_2$ formation. In either an air or an oxygen atmosphere, the favorable temperature range for crystallization of $LiNiO_2$ is between 700 and 800°C, most probably in the range 720 to 750°C.

The relation between the initial discharge capacity and the average oxidation state of $LiNiO_2$ is shown in Fig. 1. The samples with different oxidation states were obtained by adjusting the heating temperature and partial pressure of oxygen. In general, the lower the temperature and the lower the oxygen partial pressure used below 700°C, the lower was the average-degree of oxidation of the nickel. On the other hand, the higher the temperature and the longer the heating time, the higher the degree of oxidation of nickel above 800°C. The degree of oxidation which exhibited the highest discharge capacity was close to 2.95, and was obtained at 720°C in oxygen,

3.2. Thermochemistry of synthesis

In order to gain a detailed understanding of the crystalline transformation during the various synthesis condi-

Table 2
Initial capacity of $LiNiO_2$ obtained from LiOH and $Ni(OH)_2$

Atmosphere	Heating sequence	Initial charge–discharge capacity (mA h g^{-1})	Charge–discharge efficiency (%)
Air	600°C, 9 h 720°C, 15 h	152–85	55.92
Air	650°C, 24 h	55–20	36.36
Air	650°C, 12 h 700°C, 12 h	130–55	42.30
O_2	600°C, 8 h 700°C, 16 h	170–125	73.53
O_2	600°C, 9 h 720°C, 16 h	170–135	79.41
O_2	600°C, 9 h 800°C, 16 h	152–105	69.08

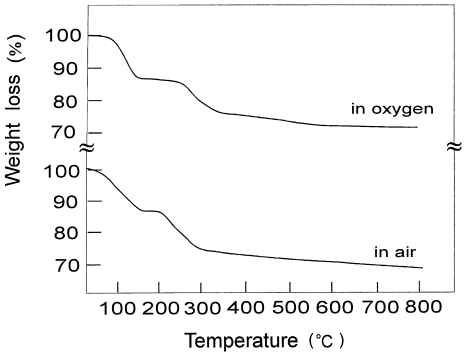

Fig. 2. TG curves for a mixture of $LiOH \cdot H_2O$ and $Ni(OH)_2$ in oxygen and in air. Scan rate: 20°C min^{-1}.

tions, TG and DSC analyses were performed on the mixture of $LiOH \cdot H_2O$ and $Ni(OH)_2$ in air and in oxygen. The TG and DSC plots are shown in Figs. 2 and 3, respectively. The first weight loss at 50 to 150°C is as high as 13.1% for the mixture in air and in oxygen. By contrast, a large endothermic peak is present in the temperature range of the DSC curve. Since this temperature cannot cause any changes in the chemical structure of $LiOH \cdot H_2O$ and $Ni(OH)_2$, but can only cause the loss of lattice water, it is reasonable to attribute the weight loss to the dehydration of $LiOH \cdot H_2O$. This assignment is further confirmed by the agreement of the calculated weight loss according to the reaction $LiOH \cdot H_2O + Ni(OH)_2 \rightarrow LiOH + Ni(OH)_2$, with the experimental value (13.1%). As the temperature is increased to 210°C, a second endothermic peak appears in the DSC plot and a weight loss of 10% is observed in the region of 210 to 300°C. It is recognized that in strongly oxidative alkaline media the hexagonal crystal $Ni(OH)_2$ is easily oxidized to the layered compound $NiO_x(OH)_{2-x}$ $(0 < x < 1)$, which is stabilized and exists as $NiO_{2/3}(OH)_{2-2/3}$ [11]. This can be written as $Ni_3O_4 \cdot 2H_2O$. At this stage, diffusion and reaction of LiOH and $Ni_3O_4 \cdot 2H_2O$ is accelerated due to the increased temperature. This leads to the formation of $LiOH \cdot NiO_{4/3}$ and is accompanied by rearrangement and dehydration of the crystal lattice. For such a reaction sequence, the expected weight loss is 9.4%, which is very close to the observed weight loss of 10%.

When temperature rises above than 300°C, the TG curve displays a very slow and gradual loss of weight; this extends to 600°C in both air and oxygen. By contract, the DSC curve exhibits an overlapping endothermic band between 450 and 500°C in both air and oxygen. This DSC feature can be explained by the fact that in this temperature region $LiOH \cdot NiO_{4/3}$ undergoes transformation to $LiNiO_2$ in two steps. First, $LiOH \cdot NiO_{4/3}$ is converted to $LiNi_{4/3}O_{4/3}(OH)$ at about 410°C, and this compound then becomes $LiNiO_2$ at 450°C with release of hydrogen and oxygen. Based on this analysis, the calculated weight loss is 5.2% and the observed weight loss was about 4.8%. This agreement supports the foregoing interpretation.

An obvious difference in both DSC and TG data appears at higher temperatures in both air and oxygen. At above 500°C, the DSC and TG data measured in oxygen display a flat straight line which indicates that neither thermochemical reaction nor weight loss is taking place. The DSC and TG data obtained in air, however, are inclined lines, which represent a continuous weight loss

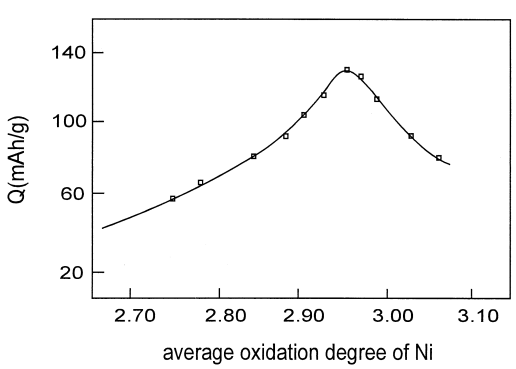

Fig. 1. Initial discharge capacity vs. the average oxidation degree of Ni for $LiNiO_2$.

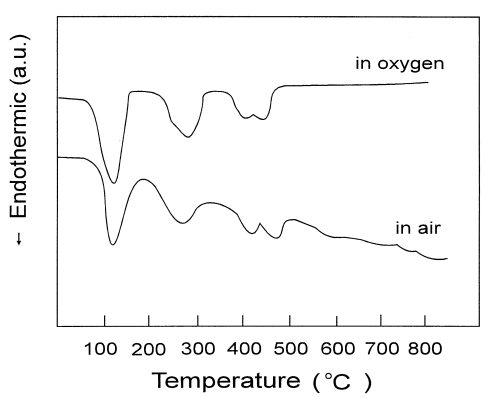

Fig. 3. DSC curves for a mixture of $LiOH \cdot H_2O$ and $Ni(OH)_2$. Scan rate: 20°C min^{-1}.

Table 3
Analysis of DSC and TG data

Suggested reaction	Calculated weight loss (%)	Measured weight loss (%)	DSC peak position (°C)
$LiOH \cdot H_2O + Ni(OH)_2$			
$\rightarrow LiOH + Ni(OH)_2$	−13.4	−13.1	115
$\rightarrow LiOH + NiO_{2/3}(OH)_{2-2/3}$	−0.5		
$(Ni_3O_4 \cdot 2H_2O)$		−10	290
$\rightarrow LiOH \cdot NiO_{4/3}$	−8.9		
$\rightarrow LiNiO_{4/3}(OH)$	−5.2	−4.8	410
$\rightarrow LiNiO_2$			450
In total	−28	−27.9	

and an endothermic reaction process. These phenomena imply that $LiNiO_2$ is not a thermally stable compound but tends to release oxygen, especially at temperatures above 500°C. Hence, in order to keep the composition and structure of the resulting $LiNiO_2$ stable, the use of an oxygen atmosphere for heat treatment is very crucial in the synthesis. A summary of the experimental data and derived reaction mechanism for $LiNiO_2$ preparation is presented in Table 3.

3.3. Electrochemical performance

The lithium intercalation properties and charge–discharge performance of $LiNiO_2$ material prepared in various ways have been described in either studies [3,12,13]. The present work focuses on the electrochemical performance of the $LiNiO_2$ synthesized from $LiOH \cdot H_2O$ and $Ni(OH)_2$.

The differential curve of dQ/dV vs. V and the cyclic voltammogram of $LiNiO_2$ are given in Figs. 4 and 5, respectively. Both curves show three pairs of oxidation–reduction peaks which are associated with the three steps of the phase formation in lithium intercalation. These results are in accordance with previous work.

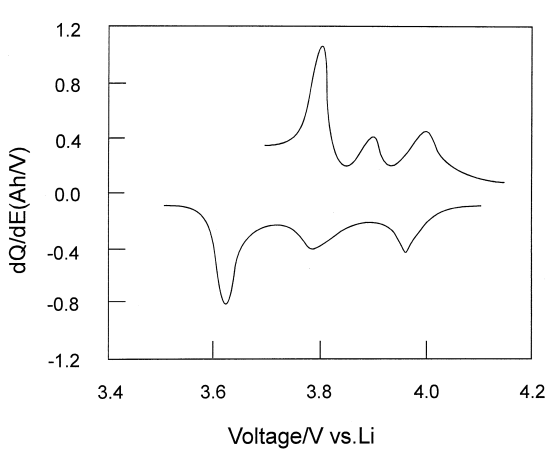

Fig. 4. Differential curve of dQ/dV vs. V from first charge–discharge curve of $LiNiO_2$ at constant current of 5 mA g^{-1}.

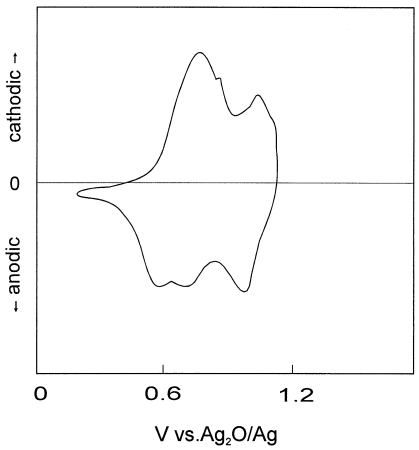

Fig. 5. Cyclic voltammograms for $LiNiO_2$ powder microelectrode. Scan rate: 2 mV s^{-1}.

The discharge curves of a $LiNiO_2$ cathode in 1 M $LiClO_4/PC + DME(1:1)$ are given in Fig. 6. For a low current of 5 mA g^{-1}, the cathode exhibits a discharge capacity of 145 mA h g^{-1}, 90% of which is delivered at > 3.5 V. When the current is increased to 25 mA g^{-1}, the voltage plateau is lowered by about 250 mV. This suggests that the high-rate capability of $LiNiO_2$ is inferior to that of $LiCoO_2$ or $LiMn_2O_4$.

The cycleability of $LiNiO_2$ is very sensitive to the depth-of-charge. For example, it can be seen in Fig. 7 that when $LiNiO_2$ is cycled to a deeper charging state corresponding to $x = 0.7$ in $Li_{1-x}NiO_2$, the charge–discharge curve exhibits severe polarization though only a few cycles was conducted. By comparison, at $x \leq 0.65$ the charge–discharge behaviour of $Li_{1-x}NiO_2$ remains almost unchanged and demonstrates the considerable reversibility for lithium insertion and extraction. This feature can also be seen in cyclic voltammograms for $LiNiO_2$ (Fig. 8). When the potential scan is limited to 0.2–1.1 V, the area and the shape of the oxidation–reduction peaks remain steady without much change with cycling. When the potential scan is extended to 1.2 V, however, the peak current rapidly decreases and the peak positions are shifted considerably and this indicates increasing polarization with cycling.

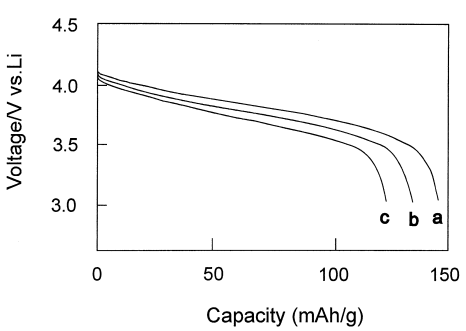

Fig. 6. Discharge curves of $LiNiO_2$ at constant current of (a) 5, (b) 15, (c) 25 mA g^{-1}.

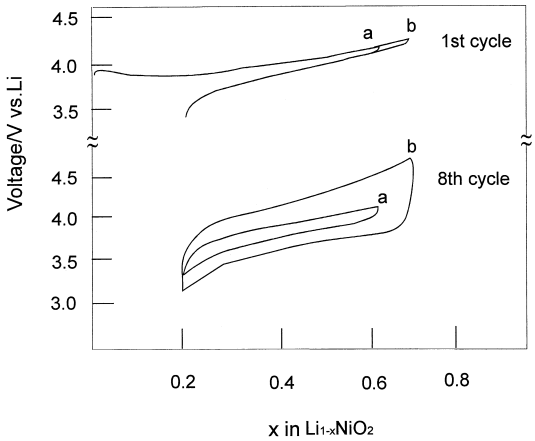

Fig. 7. Charge–discharge of x in $Li_{1-x}NiO_2$ cathode cycled at lithium composition range of (a) $0.2 \leq x \leq 0.65$ and (b) $0.2 \leq x \leq 0.70$.

In order to detect changes in the crystalline structure of $Li_{1-x}NiO_2$ with different lithium composition, XRD measurements were performed on $LiNiO_2$ cathodes cycled to different extents.

The XRD patterns of a series of $Li_{1-x}NiO_2$ cathodes with the same composition obtained by charge or discharge are presented in Fig. 9. The samples labeled 'a' represent the oxidation state $Li_{1-x}NiO_2$ obtained by directly charging $LiNiO_2$ to the required lithium composition. The samples labeled 'b' are obtained by first charging $LiNiO_2$ to $Li_{1-0.65}NiO_2$ and then discharging $Li_{1-0.65}NiO_2$ to the stated composition. It is obvious that in the region of $0.2 \leq x \leq 0.65$, $Li_{1-x}NiO_2$ cathodes with the same lithium composition have the same XRD features, despite being in the charge or discharge state. Nevertheless, when the samples are overcharged to $x \geq 0.7$, significant changes take place in the XRD spectrum of $Li_{1-x}NiO_2$. This indicates crystalline distortion or lattice transformation. In our experience, as long as a $Li_{1-x}NiO_2$ cathode is cycled in the composition range $0.2 \leq x \leq 0.65$, which corresponds to a voltage range of 3.0 to 4.1 V, a prolonged cycle life can be reached with a high discharge capacity. Under this condition, the cycling behaviour of a $Li_{1-x}NiO_2$-graphite lithium-ion battery is shown in Fig. 10. Even at constant-current charging–discharging at the 0.4 C rate, the cell provides several hundred cycles with very good rechargeability.

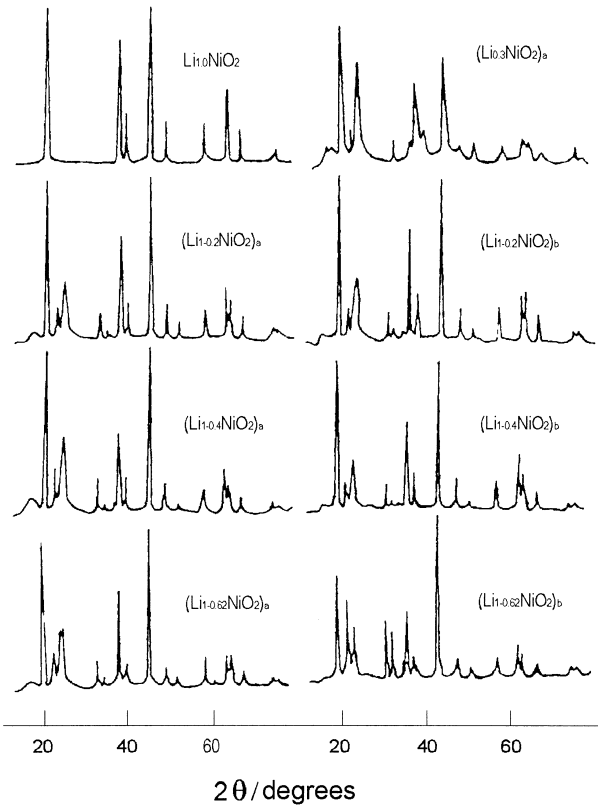

Fig. 9. XRD diffractograms for $Li_{1-x}NiO_2$ cathode at various charge–discharge depths: (a) charged state and (b) discharged state.

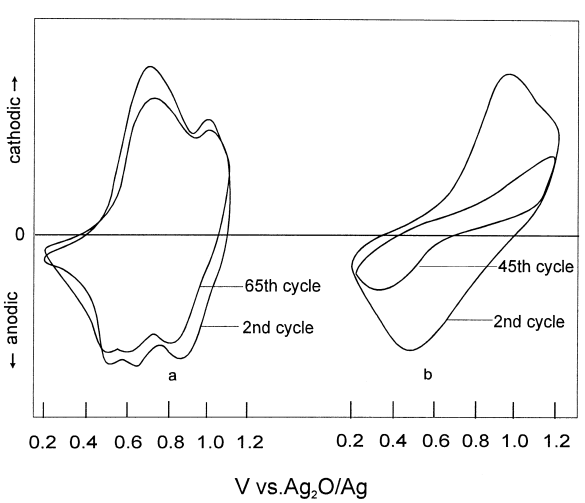

Fig. 8. Cyclic voltammograms for powder microelectrode of $LiNiO_2$ scanned over potential region of (a) 0.2–1.1 V with scan rate 2 mV s^{-1} and (b) 0.2–1.2 mV with scan rate 5 mV s^{-1}.

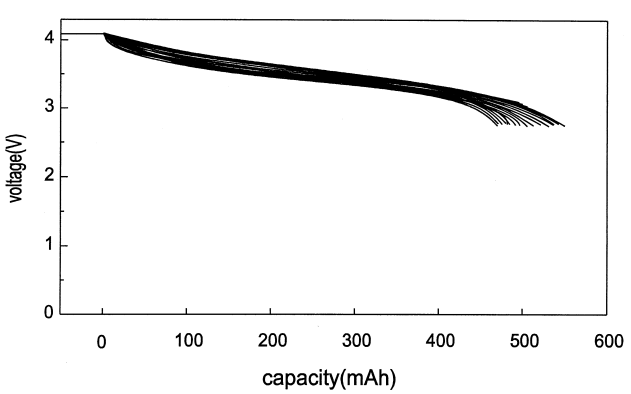

Fig. 10. Discharge curves of $LiNiO_2$ /graphite lithium-ion battery of AA size; charge–discharge current 200 mA (0.4 C).

4. Conclusions

The synthesis of $LiNiO_2$ from $Li(OH)\cdot H_2O$ and $Ni(OH)_2$ is described and the influence of the synthesis conditions on the electrochemical performance of $LiNiO_2$ is discussed. TG and DSC analyses show that the formation of $LiNiO_2$ proceeds through the transformation of $Ni(OH)_2$ to the layered compound $Ni_{1-x}(OH)_{2-x}$ followed by a solid reaction with LiOH. The optimum synthesis conditions for $LiNiO_2$ preparation is heating the mixture of $Li(OH)_2$ and $Ni(OH)_2$ at 650°C for 9 h and then at 720°C for 15 h in an oxygen atmosphere. In general, the resulting $LiNiO_2$ has a high capacity of 175 mA h g^{-1} on the first charge and 145 mA h g^{-1} on the first discharge, and sufficient cycle life when cycled over the $0.2 \leq x \leq 0.65$ composition range.

Acknowledgements

This work was supported by the National High Technology Development Project of China.

References

[1] Lecerf, M. Broussely, J.P. Gabano, Eur. Patent No. 0 345 707.
[2] Lecerf, M. Broussely, J.P. Gabano, US Patent No. 4 980 080, Dec. 12, 1989.
[3] M. Broussely, F. Perton, J. Labat, R.J. Staniewicz, A. Romero, J. Power Sources 43/44 (1993) 209.
[4] T. Ohzuku, A. Ueda, M. Nagayama, J. Electrochem. Soc. 140 (1993) 1862.
[5] R. Kanno, H. Kubo, Y. Kawamoto, T. Kamiyama, F. Izumi, Y. Takeda, M. Takano, J. Solid State Chem. 110 (1994) 216.
[6] A. Rougier, P. Gravereau, C. Delmas, J. Electrochem. Soc. 143 (1996) 1168.
[7] S. Yamada, M. Fujiwara, M. Kanda, The Seventh International Meeting on Lithium Batteries, Boston, USA, Ext. Abstr. and Program, p. 423.
[8] S. Cha, C.M. Li, H.X. Yang, P.F. Liu, J. Electroanal. Chem. 368 (1994) 47.
[9] J.R. Dahn, U. von Sacken, M.W. Juzkow, H.Al. Janaby, J. Electrochem. Soc. 138 (1991) 2207.
[10] G. Dutta, A. Manthiram, J.B. Goodenough, J. Solid State Chem. 96 (1992) 123.
[11] R.S. McEwen, J. Phys. Chem. 75 (1971) 1782.
[12] M. Broussely, F. Perton, P. Biensan, J.M. Bodet, J. Labat, A. Lecerf, C. Delmas, A. Rougier, J.P. Pérès, J. Power Sources 54 (1995) 109.
[13] C. Delmas, I. Saadoune, A. Rougier, J. Power Sources 43/44 (1993) 595.